J. Phys.: Condens. Matter **23** (2011) 115501 (5pp) doi:10.1088/0953-8984/23/11/115501

Bonding characters of Al-containing bulk metallic glasses studied by ^{27}Al NMR

X K Xi[1,2], M T Sandor[1], H J Wang[1], J Q Wang[2], W H Wang[2] and Y Wu[1]

[1] Department of Physics and Astronomy, University of North Carolina, Chapel Hill, NC 27599-3255, USA
[2] Institute of Physics, Chinese Academy of Sciences, Beijing 100190, People's Republic of China

Received 27 October 2010, in final form 1 February 2011
Published 1 March 2011
Online at stacks.iop.org/JPhysCM/23/115501

Abstract
We report very small ^{27}Al metallic shifts in a series of Cu–Zr–Al bulk metallic glasses. This observation and the Korringa type of spin–lattice relaxation behavior suggest that s-character wavefunctions weakly participate in bonding and opens the possibility of enhanced covalency (pd hybridization) with increasing Al concentration, in good agreement with elastic constants and hardness measurements. Moreover, *ab initio* calculations show that this bonding character originates from the strong Al 3p band and Zr 4d band hybridization since their atomic energy levels are closer to each other while the Al 3s band is localized far below the Fermi level. This study might provide a chemical view for understanding flow and fracture mechanisms of these bulk glass-forming alloys.

(Some figures in this article are in colour only in the electronic version)

1. Introduction

One of the crucial issues for understanding the microscopic mechanisms of plastic deformation and fracture of amorphous solids is to characterize their bonding characters. Electronic structural characteristics which are relevant for such an understanding are still insufficient [1]. *Ab initio* electronic structure calculations within the framework of density functional theory (DFT) have been used for characterizing the partial electron density of states (DOS) and charge density [2, 3]. Experimentally, on the other hand, it still remains a challenge to probe such characteristics of electronic structure through emission and absorption spectroscopic measurements on these amorphous alloys [4]. Other measurements, such as the Hall effect and the electronic specific heat, can only provide total DOS at the Fermi energy [4, 5]. The situation is different for the characterization of electronic structure via metallic shift measurements in amorphous alloys [6–8]. There is a good chance of relating metallic shifts to the s character of the DOS at the Fermi level since metallic shifts depend sensitively on the s-DOS at the Fermi energy for the atoms of interest.

In this paper, Al-bearing $(Cu, Zr)_{100-x}Al_x$ ($x = 2, 4, 6, 8, 10$) bulk metallic glasses (BMGs) are evaluated using their local DOS at the Al sites. What we found is that ^{27}Al isotropic metallic shifts of such BMGs are all very small, ~300 ppm, less than one-fifth of that in Al metal (which is 1630 ppm [6]). This observation raises the following questions: what is the origin of the small metallic shift? Is the reduced metallic shift relevant for understanding the bonding character and then the enhancement of mechanical properties such as micro-hardness upon Al alloying in these metallic glasses? We propose that probing the electronic properties of Al-centered locally favored structures in these metallic glasses by ^{27}Al nuclear magnetic resonance (NMR) is an effective step towards answering the above questions. The small ^{27}Al metallic shifts originate from the low s-DOS at the Fermi energy at Al sites. The BMG will exhibit enhanced micro-hardness if there is an appreciable pd hybridization from dissimilar constituent elements in the vicinity of the Fermi level.

2. Experimental details

Systematic investigations were carried out on a metallic glass system $(Cu_{0.5}Zr_{0.5})_{100-x}Al_x$ ($x = 2, 4, 6, 8, 10$) which shows a strong compositional dependence of micro-hardness and plasticity [9–11]. BMG cylinders 2 mm in diameter were fabricated by conventional copper mold

casting. Their amorphous nature was characterized by x-ray diffraction and confirmed by differential scanning calorimetry. Glassy cylinders were then crushed into powders for NMR experiments. All NMR measurements were performed in a magnetic field of 7.01 T. The rf pulse strength ω_{rf} was calibrated using several methods [12]. 1 M $Al(NO_3)_3$ aqueous solution was used to calibrate the metallic shift and determine the 90° pulse length (t_p) for the liquid with the property $\omega_{rf}t_p = \pi/2$. The ^{27}Al NMR signal was recorded using a two-pulse Hahn echo sequence [13]. A typical rf field strength of $\omega_{rf}/2\pi = 100$ kHz was used for the detection of the spectrum. The measured full width at half-maximum of the central line associated with the central transition $|-1/2\rangle \leftrightarrow |+1/2\rangle$ is ~30 kHz for all the BMGs. Signal averaging was carried out with a recycle delay of 150 ms. The spin–lattice relaxation time (T_1) measurements were carried out using the saturation recovery method [17] with $\omega_{rf}/2\pi = \sim 12$ kHz for the selective excitation of the central transition only. All the spectra are mapped as a Fourier transform of the spin echo signal.

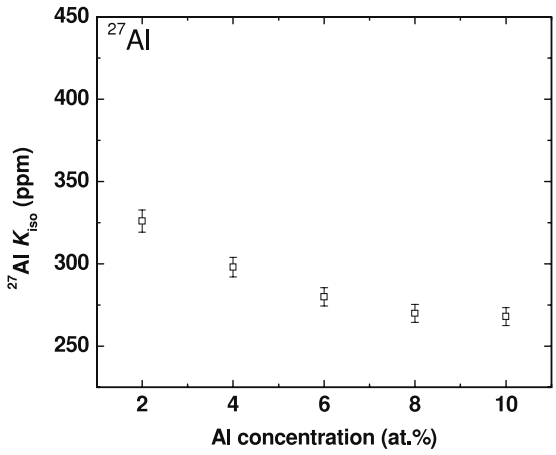

Figure 1. ^{27}Al isotropic metallic shifts versus Al concentration in $(Cu, Zr)_{100-x}Al_x$ ($x = 2, 4, 6, 8, 10$) metallic glasses measured at 298 ± 2 K.

3. Results and analysis

Figure 1 shows the ^{27}Al isotropic metallic shifts as a function of Al concentration in the $(CuZr)_{100-x}Al_x$ glass system measured at 298 K. The most striking feature is that the observed ^{27}Al isotropic metallic shifts are rather small, i.e. of the order of ~300 ppm for all the samples and less than one-fifth of that for pure Al metal (~1630 ppm), indicating the s character of the DOS at Al sites at the Fermi energy is very small. Instead of increasing, the isotropic ^{27}Al metallic shifts decreases slightly from 320 ppm for $x = 2$ to 280 ppm for $x = 10$. This reveals the immediate structural environment of Al is changing with the nominal composition. The overall very small metallic shift indicates the lack of Al–Al chemical correlation pairing in these metallic glasses within the glass-forming range, consistent with similar observations in Cu–Zr–Al glass-forming alloys [14, 15]. A smooth variation of the metallic shift with Al concentration suggests the absence of any minimum in the local density of states at Al sites at the Fermi energy within the investigated composition range.

The total ^{27}Al NMR shifts in weakly paramagnetic or non-magnetic metals can be described as [16] $K_{total} = K_s + K_{orb} + K_d + K_{cs}$, where K_s is the direct contact shift reflecting the magnetic coupling of the nucleus to the s character of conduction electrons, which is usually the dominant contribution in metals; K_{orb} is the orbital shift originating from the orbital angular momentum, mainly from the d character of conduction electrons; and K_d refers to the shift from the contribution of the d character of the conduction electrons via spin core polarization. The chemical shift K_{cs} is usually much smaller than K_s in metals. However, K_{cs} is significant in the analysis of the total shift when K_s becomes very small.

The ^{27}Al shifts of all these BMGs show temperature invariance between 77 and 300 K, in agreement with the magnetic susceptibility measurements for these non-magnetic BMGs [29]. To see more clearly what is responsible for the observed very small ^{27}Al metallic shifts, spin–lattice relaxation times (T_1) were performed at various temperatures. If a quadrupole interaction is involved, the spin–lattice relaxation is no longer of a single-exponential form, as for the simple case of spin $I = 1/2$ nuclei. The quadrupole interaction results in unequally spaced atomic energy multi-level systems. In that case, the resulting saturation recovery magnetization $M^*(t)$ profiles can be fitted well with a multi-exponential function [17, 18]:

$$\frac{M^*(t) - M_0}{M_0} = -2\alpha\left[0.257\exp\left(-\frac{t}{T_1}\right) + 0.267\exp\left(-\frac{6t}{T_1}\right) + 0.476\exp\left(-\frac{15t}{T_1}\right)\right], \quad (1)$$

where t is the recovery time, α is a fractional number derived from initial conditions and M_0 is the fully recovered magnetization. The measured room temperature T_1s for the BMGs are approximately ~100 ms, one order of magnitude longer than ~6 ms of pure Al metal [6]. The spin relaxation rate $1/T_1$ can be written as [19]

$$1/T_1 = 4\pi\hbar k_B T[\gamma_n H_{hf}^s g_s(E_f)]^2 + [\text{non-s}] + [\text{quadrupole moment}], \quad (2)$$

where h, k_B and T are the reduced Planck constant, Boltzmann constant and absolute temperature, respectively. γ_n is the gyromagnetic ratio of the Al nucleus. H_{hf}^s is the hyperfine field per electron of the Al s electrons at the Fermi level. $g_s(E_f)$ represents the s-DOS at the Fermi level. From equation (2), it is straightforward that, if the first contact term due to the Fermi contact hyperfine interaction is not much increased by correlation and exchange, the measured relaxation time can only be less than that given by the first term alone and all other relaxation contributions always shorten the relaxation time [6]. The observed much longer T_1 clearly demonstrates the $g_s(E_f)$ is much smaller than that in Al metal! Figure 2 clearly shows the spin–lattice relaxation follows a Korringa type of behavior [20], with $T_1T = 29 \pm 1$ (s K) over the temperature interval from 77 to 300 K for a typical $Cu_{46}Zr_{46}Al_8$ BMG. This Korringa relaxation behavior means that the orbital

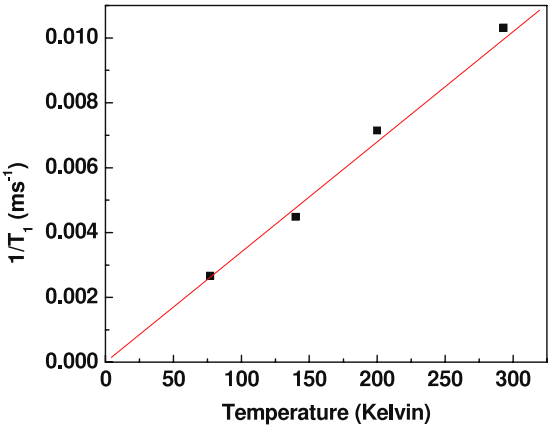

Figure 2. ^{27}Al spin–lattice relaxation rate ($1/T_1$) plotted against temperature (T) for $Cu_{45}Zr_{45}Al_{10}$ metallic glass. The red solid line is a fit to T_1 with $T_1T = 29 \pm 1$ (s K).

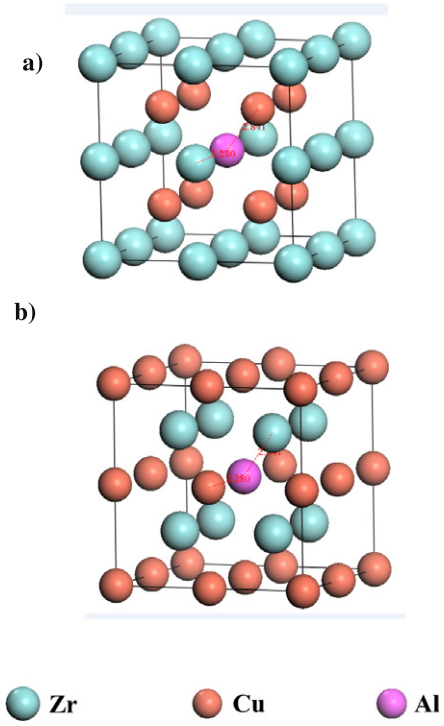

Figure 3. B2 structural representations: (a) $Cu_8Zr_7Al_1$ with the Al atom surrounded by Cu atoms and (b) $Cu_7Zr_8Al_1$ with the Al atom surrounded by Zr atoms.

contributions can be neglected [16]. The specific heat and susceptibility data [29] indicate a considerable decrease in the d DOS at the Fermi energy, $g_d(E_f)$, upon the addition of Al. If we assume K_d dominates, due to the cancellation of K_d (K_d is negative) [19], the ^{27}Al metallic shift would have been expected to increase upon Al alloying since the negative contribution via spin core polarization depends on $g_d(E_f)$ and the cancellation becomes smaller when $g_d(E_f)$ decreases in the case of more addition of Al. This is not consistent with the experimentally observed decreasing ^{27}Al metallic shift as a function of Al concentration, as shown in figure 1. The contribution from K_d can thus be neglected here. From the Korringa relation, $T_1TK^2 = f\frac{\hbar}{4\pi k_B}\frac{\gamma_e^2}{\gamma_n^2} = 3.872\,97 \times 10^{-6} f$ [s K], where γ_e is the gyromagnetic ratio of the electron. The estimated enhancement factor f value is 0.6, indicating the Fermi contact interaction with s-conduction electrons causes both K and $1/T_1$, which demonstrates that exchange effects resulting from d-electron couplings are insignificant [6]. Because of the lack of many unknown hyperfine coupling parameters, a full explanation of the observed small metallic shifts and spin–lattice relaxation times is not possible at this time. Nevertheless, the above line of reasoning strongly suggests that the observed very small ^{27}Al metallic shifts should mainly be attributed to the low $g_s(E_f)$.

Two possible mechanisms are proposed to be responsible for the observed low s character $g(E_f)$: one is the Hume-Rothery-like pseudogap mechanism [2] and the other is the concept of covalent bonding via hybridization [21]. In the nearly-free-electron model, when the Fermi wavenumber k_F satisfies $k_F \approx \boldsymbol{k}_p/2$, where $\boldsymbol{k}_p$ is the position of the first peak in the structure factor which can be determined by diffraction techniques, the Fermi energy is located at the pseudogap of the sp band which is thus interpreted as the geometric origin [22]. In terms of extended Faber–Ziman theory, the condition $k_F \approx \boldsymbol{k}_p/2$ is fulfilled for most liquid and amorphous alloys [23]. This Hume-Rothery-like pseudogap idea supports the observed small metallic shift results. However, this idea alone cannot fully explain the small and decreasing ^{27}Al metallic shifts upon Al alloying in $(Cu, Zr)_{100-x}Al_x$ BMGs. For elements with different chemical natures, the chemical effects might also play an important role in the formation of low $g_s(E_f)$. *Ab initio* calculations within DFT were also implemented in the Vienna *ab initio* simulation package (VASP) code [24], which clearly show that chemical effects are also responsible for the observed low $g_s(E_f)$. We start from B2-CuZr as a structural model. The composition of this intermetallic compound is consistent with the ratio of Cu to Zr for the BMGs under study. For the addition of Al, we generated a $2 \times 2 \times 2$ supercell of B2-CuZr with eight Cu and eight Zr. Two separate structures were created where one Zr or one Cu atom is substituted with one Al atom, resulting in Cu_8Zr_7Al and Cu_7Zr_8Al that are close in composition to $(Cu, Zr)_{92}Al_8$ in this study (see figure 3). Figure 4 shows the total and angular momentum decomposed DOS at Al sites of Cu_8Zr_7Al, and Cu_7Zr_8Al. The $g_s(E_f)$, for pure Al, Cu_8Zr_7Al and Cu_7Zr_8Al are 0.045, 0.010 and 0.002 states eV^{-1} atom, respectively. Since the Wigner–Seitz radii of the Al atoms were set equally, the $g_s(E_f)$ of Al is proportional to $\langle|\psi_s(0)|^2\rangle_{E_F}$. The relatively low values of $g_s(E_f)$ observed in Cu_7Zr_8Al and Cu_8Zr_7Al are strong indications that small ^{27}Al metallic shifts are due to small $\langle|\psi_s(0)|^2\rangle_{E_F}$. The increase in the distance between Al atoms in these structures yields a narrowing of their bandwidths compared to those in pure Al metal, as shown in figure 4. The Al 3s does not hybridize with the Zr s or Cu s states due to the large differences in atomic energy levels between Al 3s and Zr 3s by -3.3 eV, and between Al 3s and Cu 3s by -3.1 eV. Hybridization takes place among the Al 3p, Zr 4d and Cu 3d bands due to their close proximity in energy. Then the Al 3s and 3p do not hybridize as they do in pure Al metal due to

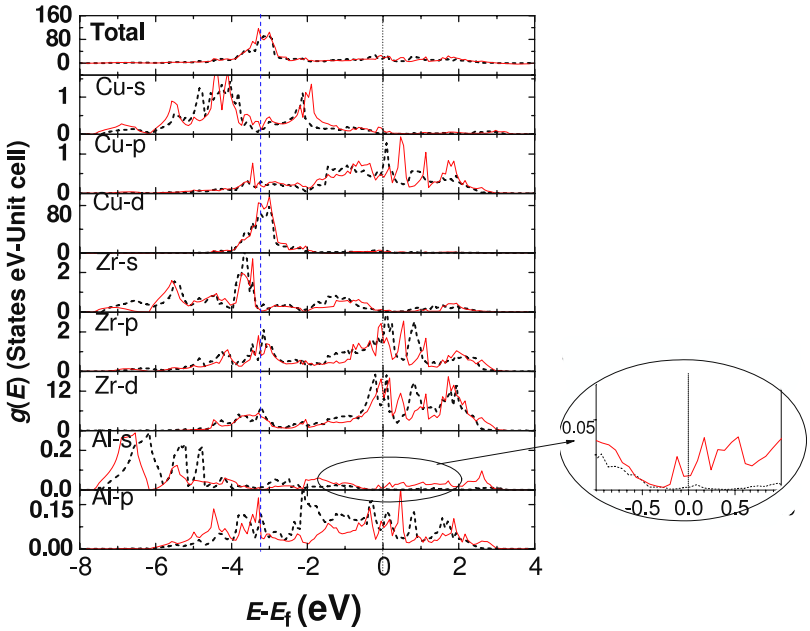

Figure 4. Self-consistently calculated s, p and d partial density of states for $Cu_7Zr_8Al_1$ (black dashed line) and $Cu_8Zr_7Al_1$ (red solid line) with B-2 structure.

the narrowing of the bandwidth. In Cu_8Zr_7Al, where Al is surrounded by Cu, the Al s band is maximized at −6.5 eV and spreads across the Fermi level from −7.6 to 3 eV. In contrast, when Al is surrounded by Zr(Cu_7Zr_8Al), the s band (−7.3 to −0.5 eV, maximized at −6.2 eV) is narrower and does not spread across the Fermi level. Most of the Al s electrons in Cu_7Zr_8Al therefore do not participate in the conduction band, but rather are localized around Al sites in the BMGs, as shown in figure 4. Both structural models generate similar structures in the valence band that has a much lower $g_s(E_f)$ than that of Al metal. The chemical effects can be responsible for the even lower $g_s(E_f)$ for Cu_7Zr_8Al, in which Al is surrounded by Zr. This is due to the difference in the chemistry of Cu and Zr. This observation of dehybridization of sp wavefunctions and localization of s electrons at higher binding energy is in accordance with previous simulations in metallic glasses such as Al 3s in Ca–Al [25], B 2s and P 3s in Fe–B and Fe–P [26], and Si 3s in Pd–Si [27] metallic glasses. Now, it is clear that the origin of the observed very small ^{27}Al metallic shifts for $(Cu, Zr)_{100-x}Al_x$ is primarily attributed to the fact that the wavefunction of s character is depleted at Al sites at the Fermi level while it is localized below the Fermi level. The bands which cross the Fermi level are mainly the Zr 4d states, in good agreement with the x-ray photoemission and Hall coefficient results of the CuZrAl alloy system [28] and also in agreement with the decreasing magnetic susceptibility and specific heat coefficients measured at low temperatures in CuZrAl metallic glasses as a function of Al concentration [29].

Implications can be found from the above results. According to Friedel's model of cohesion [30], the bond energy for a transition-metal-based alloy is affected by pd hybridization. The gain of hybridization with Al addition increases the cohesive energy and thus changes the hardness. In general, the micro-hardness should get larger when adding more Al concentration since more Al–TM pairs will be obtained. This analysis is consistent with the recent micro-hardness measurement within the glass-forming composition range [11]. On the other hand, pd hybridization between Al and TM atoms will introduce directional bonds and the BMGs will be expected to exhibit brittleness if Al–TM pairs with directional bonding percolate, or plasticity if the electronic configuration is mostly s-like since the bonding will be more non-directional in this case.

4. Conclusions

In summary, this work reports NMR evidence of very low Al 3s DOS near the Fermi energy and that the 3s levels of Al are located well below the Fermi energy in Zr–Cu–Al glasses. The calculated partial s-DOS shows reasonable agreement with the experimental measurements. Furthermore, pd hybridization between Al and transition metal atoms is proposed to be responsible for this observation, which links the origin of the small ^{27}Al metallic shifts to the covalent-like bonding character in these glass-forming alloys. This study provides an atomic and electronic basis for further understanding their macroscopic properties.

Acknowledgments

Comments on calculations by W M Mullins are gratefully acknowledged. Financial support for this project was provided by the US Army Research Office (grant no. W911NF-09-1-0343), China NSF (50621061 and 51071171) and the Chinese Academy of Sciences.

References

[1] Miracle D B, Egami T, Flores K M and Kelton K F 2007 *MRS Bull.* **32** 629

[2] Hafner J 1981 Glassy metal I: ionic structure, electronic transport, and crystallization *Theory of the Structure, Stability, and Dynamics of Simple-Metal Glasses* ed H-J Guntherodt and H Beck (Berlin: Springer)

[3] Ogata S, Li J and Yip S 2002 *Science* **298** 807

[4] Johnson W L and Tenhover M 1983 Glassy metals *Magnetic, Chemical, and Structural Properties* ed R Hasegawa (Boca Raton, FL: CRC Press)

[5] Mizutani U 1983 *Prog. Mater. Sci.* **28** 97

[6] Slichter C P 1996 *Principles of Magnetic Resonance* corrected 3rd edn (Berlin: Springer)

[7] Lashmore D S, Bennett L H, Schone H E, Gustafson P and Watson R E 1982 *Phys. Rev. Lett.* **48** 1760

[8] Eckert H 1992 *Prog. Nucl. Magn. Reson. Spectrosc.* **24** 159
Tang X P, Loffler J F, Johnson W L and Wu Y 2003 *J. Non-Cryst. Solids* **317** 118

[9] Yu P, Bai H Y and Wang W H 2006 *J. Mater. Res.* **21** 1674

[10] Zhang Q S, Zhang W, Xie G Q and Inoue A 2007 *Mater. Trans.* **48** 1626

[11] Cheung T L and Shek C H 2007 *J. Alloys Compounds* **434** 71

[12] Xi X K, Li L L, Zhang B, Wang W H and Wu Y 2007 *Phys. Rev. Lett.* **99** 095501

[13] Hahn E L 1950 *Phys. Rev.* **80** 580

[14] Cheng Y Q, Ma E and Sheng H W 2009 *Phys. Rev. Lett.* **102** 245501

[15] Wang X D, Jiang Q K, Cao Q P, Bednarcik J, Franz H and Jiang J Z 2008 *J. Appl. Phys.* **104** 093519

[16] Hines W A, Glover K, Clark W G, Kabacoff L T, Modzelewski C U, Hasegawa R and Duwez P 1980 *Phys. Rev.* B **21** 3771

[17] McDowell A F 1995 *J. Magn. Reson.* A **113** 242

[18] Lue C S, Lin J Y and Xie B X 2006 *Phys. Rev.* B **73** 35125

[19] Rowland T J 1961 *Prog. Mater. Sci.* **9** 3

[20] Korringa J 1950 *Physica* **16** 601

[21] Nozawa K and Ishii Y 2010 *Phys. Rev. Lett.* **104** 226406

[22] Trambly de Laissardière G, Nguyen-Manh D and Mayou D 2005 *Prog. Mater. Sci.* **50** 679

[23] Samwer K and Vonlohneysen H 1982 *Phys. Rev.* B **26** 107

[24] Kresse G and Furthmüller J 1996 *Phys. Rev.* B **54** 11169

[25] Nagel S R *et al* 1982 *Phys. Rev. Lett.* **49** 575

[26] Fujiwara T 1982 *J. Phys. F: Met. Phys.* **12** 661

[27] Riley J D, Ley L, Azoulay J and Terakura K 1979 *Phys. Rev.* B **20** 776

[28] Mizutani U, Yamada Y, Matsuda T and Mishima C 1987 *Solid State Commun.* **62** 641

[29] Li Y, Bai H Y, Wang W H and Samwer K 2006 *Phys. Rev.* B **74** 052201

[30] Friedel J 1969 Transition metals. Electronic structure of the *d*-band. Its role in the crystalline and magnetic structures *The Physics of Metals* ed J M Ziman (London: Cambridge University Press)